Tectonics

RESEARCH ARTICLE
10.1029/2018TC005297

Key Points:
- The fluid-induced eclogitization on Holsnøy is controlled both dynamically by shear zone development and static equilibration
- Eclogite-facies shear zone geometry on Holsnøy is scale-independent from centimeter to kilometer scale

Supporting Information:
- Supporting Information S1

Correspondence to:
S. Zertani,
sascha.zertani@fu-berlin.de

Citation:
Zertani, S., Labrousse, L., John, T., Andersen, T. B., & Tilmann, F. (2019). The interplay of eclogitization and deformation during deep burial of the lower continental crust—A case study from the Bergen Arcs (western Norway). *Tectonics*, *38*, 898–915. https://doi.org/10.1029/2018TC005297

Received 23 AUG 2018
Accepted 1 FEB 2019
Accepted article online 6 FEB 2019
Published online 7 MAR 2019

The Interplay of Eclogitization and Deformation During Deep Burial of the Lower Continental Crust—A Case Study From the Bergen Arcs (Western Norway)

Sascha Zertani[1], Loic Labrousse[2], Timm John[1], Torgeir B. Andersen[3], and Frederik Tilmann[1,4]

[1]Institute of Geological Sciences, Freie Universität Berlin, Berlin, Germany, [2]Sorbonne Université, CNRS-INSU, Institut des Sciences de la Terre Paris, ISTeP, UMR 7193, Paris, France, [3]The Centre of Earth Evolution and Dynamics (CEED), Department of Geosciences, University of Oslo, Oslo, Norway, [4]Deutsches GeoForschungsZentrum, Potsdam, Germany

Abstract The island of Holsnøy in the Bergen Arcs, which belong to the Caledonides of western Norway, represents an excellent example of how fluid-induced eclogitization modifies material deeply buried by subduction and continental collision. We produced a new detailed map of the northwestern part of Holsnøy, differentiating not only the magnitude of eclogitization but also the strain intensity at different spatial scales: from the outcrop to the entire massif. Using structural data from eclogite-facies shear zones and eclogitized low-strain domains, we show that fluid-mediated eclogitization not only progresses via the development of shear zones (dynamic eclogitization) but occurs over large areas of the island without associated deformation, creating a characteristic static eclogite-facies overprint. Static eclogitization preserves the structural features of the granulitic protolith while the rock body is transformed from a granulite- to an eclogite-facies mineral assemblage. The extent of static eclogitization was underestimated strongly in the past, a finding also relevant for the interpretation of seismological images in currently active orogens, where presumably similar processes are currently occurring. In addition, we find that the general structure of the eclogite-facies shear zones is scale-independent over several orders of magnitude. Although crustal-scale eclogite-facies complexes are rarely preserved without significant modification during exhumation, this implies that similar geometrical configurations are likely produced at the scale of the whole lower crust during subduction or continental collision and therefore shape the crustal geophysical signature.

1. Introduction

Subduction-related deformation and metamorphism are processes that cannot be studied directly or by in situ techniques. Since they take place at great depths and occur on large spatial and temporal scales, they require extrapolation over several orders of magnitude from laboratory-scale experiments. Geophysical imaging methods (e.g., seismic tomography, receiver function imaging, and observations of shear wave splitting) and deformation monitoring methods (e.g., GNSS-based observations of surface deformation or observations of seismicity) applied to active subduction systems provide insight into the large-scale processes and structures. Studies on rocks subducted in the past and now exposed at the Earth's surface provide an opportunity to study processes and structures across a range of scales. Although such exposures are rare, they not only are essential for studying the processes taking place during subduction but can also support the interpretation of large-scale geophysical images of currently active subduction and collision zones (e.g., western Hellenic arc, the Himalaya, the Cascadia subduction zone, or the Pamir; Bostock et al., 2002; Halpaap et al., 2018; Kufner et al., 2017; Labrousse et al., 2010).

In order to understand how subducted rocks react to dynamically changing pressure, temperature, and stress conditions at depth, many studies have focused on areas where partial to complete eclogitization has modified the downgoing material (e.g., Austrheim, 1987; John & Schenk, 2003; Wain et al., 2001). It has been shown that the presence of a fluid phase is crucial for the transformation of crustal rocks to eclogite-facies assemblages (Austrheim, 1987; John & Schenk, 2003; Mørk, 1985; Wayte et al., 1989). Additionally, examples from the Western Gneiss Region and the Bergen Arcs in the Caledonides show that ongoing deformation during metamorphism plays a major role in eclogite formation (e.g., Austrheim, 2013; Wain et al., 2001). While fluid-mediated eclogitization can be facilitated by deformation (Austrheim, 1987), John and Schenk (2003) suggested that the main mechanisms that contributed to eclogite formation in the Zambezi Belt are

fluid-mediated dissolution, transport, and precipitation processes; consequently, nanoscale to microscale processes may lead to eclogitization without associated deformation (static eclogitization) also on a macroscopic scale (Putnis & John, 2010). However, these studies also report that while one eclogitization mechanism is dominant, the other also contributes to the eclogitization process, that is, minor static eclogitization in the Bergen Arcs and Western Gneiss Region as well as minor eclogite-facies shear zones in the Zambezi Belt (Austrheim, 1987; John & Schenk, 2003). These observations demonstrate a complex interplay between different mechanisms of eclogite formation.

The impact of deformation accompanied metamorphism becomes evident when comparing exposures of previously buried complexes to currently active subduction and collision zones. Syn-kinematic eclogites, or deformed metamorphic rocks in general, exhibit different features in terms of fabric and bulk properties compared to those formed statically, i.e., shape and crystallographic orientations or the distribution of minerals throughout the rock (e.g., Austrheim & Griffin, 1985; Boundy et al., 1992; Godard & van Roermund, 1995; Keppler et al., 2015). These features in turn potentially influence the signature of these structures in seismic images and other geophysical observables (e.g., Fountain et al., 1994; Keppler et al., 2017; Zhong et al., 2014). Specifically, eclogites typically have a higher rigidity and density compared to crustal rocks, resulting in high velocities and a low impedance contrast with respect to mantle rocks. Furthermore, they generally only develop weak to moderate rock fabrics resulting in low bulk rock anisotropy (Bascou et al., 2001; Lloyd et al., 2011; Motra & Zertani, 2018; Zhong et al., 2014). Additionally, it is important to understand if and how these structural features vary over different scales, because many of the structural relationships exposed in the field are too small to be directly observable by the geophysical imaging techniques applicable on crustal scale (e.g., Lloyd et al., 2011) but might affect the bulk properties visible at larger scale through a structurally complicated crust acting as an effective medium. Hence, a deeper understanding of scale dependence and the variability of structures over different scales is essential.

The island of Holsnøy in the Bergen Arcs of western Norway has been studied extensively (e.g., Austrheim, 1987; Austrheim & Griffin, 1985; Bhowany et al., 2017; Boundy et al., 1992; Jamtveit et al., 2018; Raimbourg et al., 2005) because it provides rare insights into partial eclogitization and associated deformation during deep burial. Previous studies have shown convincingly that brittle deformation enables fluid infiltration which leads to ductile deformation during equilibration at eclogite-facies *P-T* conditions. Notably, those parts of the buried material that are not infiltrated by fluids and remain dry escape both petrological and structural modification (Austrheim & Griffin, 1985; Boundy et al., 1992; Jamtveit et al., 1990).

Due to the exceptional exposures on Holsnøy, many parts of the island have been mapped in detail (Boundy et al., 1992; Raimbourg et al., 2005; Schmid et al., 1998). Previous studies commonly categorize the exposed complex and often transitional lithologies into three main groups: (1) high-strain areas with >80% eclogitization (eclogite), (2) low-strain areas with <40% eclogitization (granulite), and (3) the so-called eclogite breccia with 40–80% eclogitization. This categorization therefore strictly ties the petrological transition from granulite to eclogite to the structural transition from undeformed to strongly sheared rocks (Austrheim, 1990).

In this study we show that using the orientation of preserved granulite blocks and the orientation of the granulite-facies and eclogite-facies foliations within the so-called eclogite breccia, this link between deformation and petrological transitions can be relaxed, in particular by distinguishing deformation-related eclogitization and static eclogitization. A detailed map of a ~5 × 3 km^2 area on western Holsnøy based on these new criteria demonstrates how the interplay between fluid infiltration and deformation shapes the fabric and petrology of the lower crustal rocks during deep burial. Further, we discuss that the geometrical distribution of the rocks on Holsnøy is scale-independent, at least in a qualitative sense.

2. Geological Setting

The Scandinavian Caledonides that extend along the western coast of Norway are the result of the closure of the Iapetus Ocean and the Scandian continental collision stage of Baltica and Laurentia between ca. 430 and 400 Ma (Roberts, 2003). Baltica and its hyperextended pre-Caledonian margin represented the lower plate during collision (Andersen, Jamtveit, et al., 1991; Andersen et al., 2012; Corfu et al., 2014; Hacker et al., 2010; Krogh, 1977).

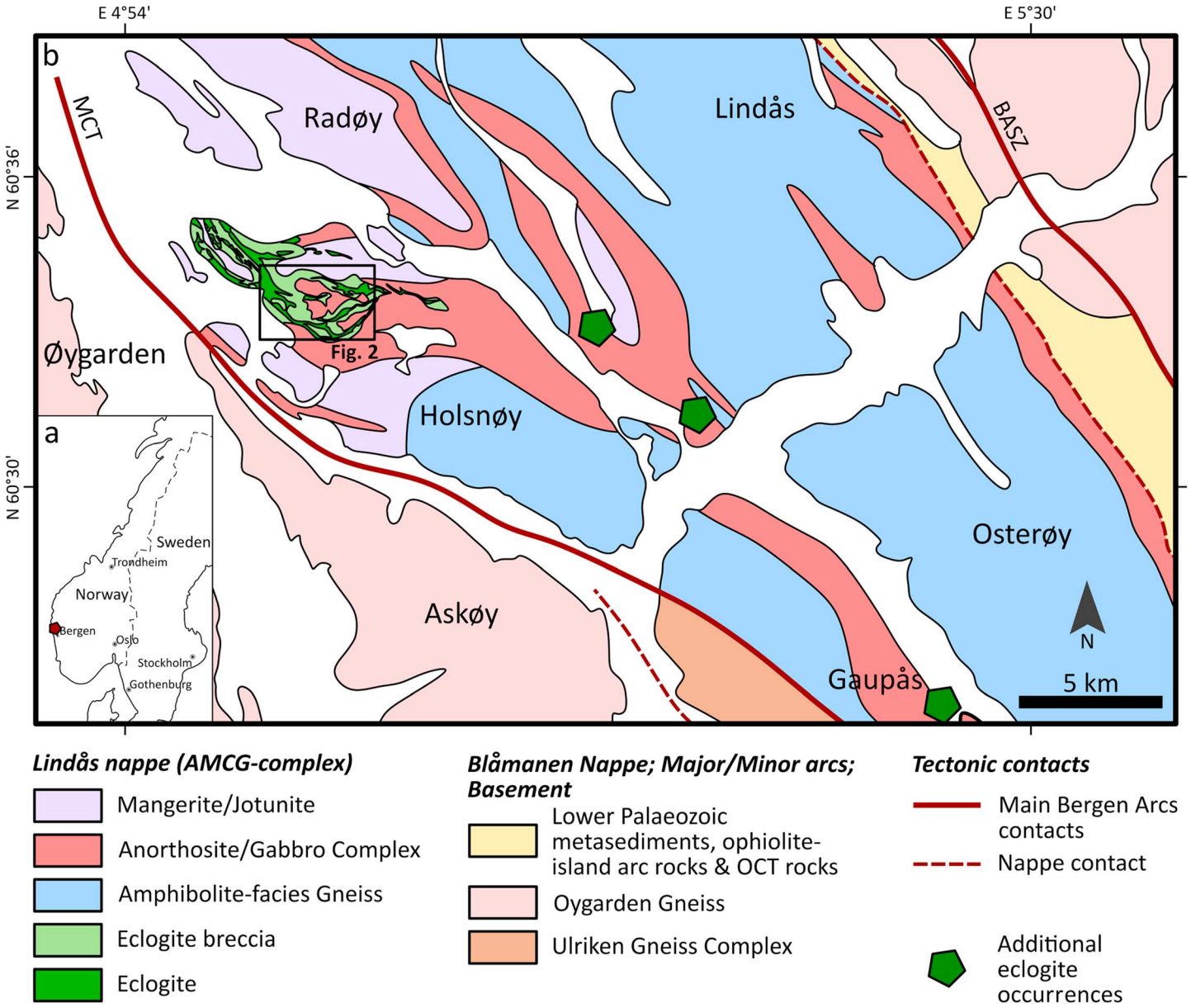

Figure 1. Geological map showing the north-central part of the Bergen Arcs with emphasis on the Lindås Nappe (for location see star in a). The map shows the dominating lithologies in the area, the strongly eclogitized northwestern part of Holsnøy and additional eclogite occurrences in the Lindås nappe (compiled from Austrheim, 2013; Centrella et al., 2015; Raimbourg et al., 2005). The black box shows the location of Figure 2. BASZ = Bergen Arcs shear zone, MCT = Main Caledonian Thrust.

The Bergen Arcs of western Norway comprise a curved nappe complex that is centered on the city of Bergen. It is composed of nappes that originated from the former Iapetus Ocean as well as the pre-Caledonian margin of Baltica. The nappes were thrusted southeastward onto Baltica during the Caledonian orogeny (Fossen & Dunlap, 1998; Roberts & Gee, 1985; Sturt et al., 1975). One of these, the Lindås nappe and its continuation into the Jotun and Dalsfjord nappe complexes, is considered to be derived from the lower crust of a former microcontinent or continental sliver along the hyperextended magma-poor segment of the pre-Caledonian margin of Baltica (Andersen et al., 1998, 2012; Austrheim, 1987; Corfu et al., 2014; Jakob et al., 2017).

The rocks exposed on the island of Holsnøy and in the Lindås nappe have a long magmatic and metamorphic history. The nappe is mostly composed of anorthosites and associated magmatic rocks, including gabbroic anorthosites, gabbros, norites, jotunites, and mangerites (Griffin, 1972; Roffeis et al., 2012). This magmatic

complex, with lithologies typically referred to as AMCG-suite rocks (anorthosite, mangerite, charnockite, granite; Austrheim & Griffin, 1985; Figure 1), initially intruded into mid- to lower crustal levels, in various magmatic pulses starting at 1.2 Ga and associated intrusions continued until ~950 Ma (Bingen et al., 2001). In the following, the complex was modified by a granulite-facies event at ~930 Ma (Bingen et al., 2001), with peak *P-T* conditions of ~1 GPa and ~850 °C (Austrheim & Griffin, 1985).

The pressure-temperature-path of the rocks in the following ~500 Ma remains poorly constrained. However, the rocks most likely cooled at lower crustal levels down to an average geothermal gradient of mid to lower continental crust (e.g., Jamtveit et al., 1990). In any case, the rocks show no signs of significant retrogression, and the mineral assemblage was not significantly modified from the mid-Proterozoic formation until Caledonian burial and reworking (e.g., Austrheim, 1987). Both the Dalsfjord and Jotun nappe complex are nonconformably overlain by Late Proterozoic to Early Paleozoic rift-related sediments (Jakob et al., 2017).

During the early stages of the Scandian Caledonian continental collision, the rocks of the Lindås-Dalsfjord-Jotun microcontinent/continental sliver were buried to eclogite-facies conditions, reaching peak pressures and temperatures at 430 ± 3.5 Ma (Glodny et al., 2008), and were subsequently partially eclogitized (Austrheim, 1987; Austrheim & Griffin, 1985). Peak metamorphic conditions were determined to be 650–750 °C and 1.7–2.1 GPa (Altenberger & Wilhelm, 2000; Bhowany et al., 2017; Jamtveit et al., 1990; Kühn et al., 2002; Raimbourg et al., 2007). Eclogitization occurred both in shear zones that developed from fractures and in small patches that remained unaffected by ductile deformation (Austrheim, 1987; Jamtveit et al., 1990). In both cases, eclogitization was induced by fluids and produced a hydrous eclogite-facies mineral assemblage (e.g., zoisite, phengite in addition to garnet and omphacite; Austrheim, 1987). The fluid source remains disputed, the Lindås-Jotun-Dalsfjord nappe complex (Jakob et al., 2017) was however thrust onto the transitional, hyperextended crust that separated the microcontinent/continental sliver from the Baltic mainland, and this overridden basin therefore is a good candidate for the source of the hydrous fluids. The impermeable nature of these dry orthogneisses, however, prevented pervasive hydration leaving large rock volumes unaffected, resulting in the complex mixture of granulites and eclogites preserved today (Austrheim & Griffin, 1985). The composition of the fluid has been studied by previous authors. Andersen et al. (1990) suggested that the fluid was N_2- and H_2O-rich using fluid inclusion studies, while Boundy et al. (2002) conclude that there might have been multiple events of fluid infiltration introducing fluids of different compositions. It is, however, clear that the dominant fluid was aqueous since the eclogitization reactions are distinctly linked to hydration processes.

The rocks were later subjected to retrogressive alteration in the amphibolite-facies (Altenberger, 1997; Austrheim & Robins, 1981; Bingen et al., 2004; Centrella et al., 2015; Glodny et al., 2008). The dynamics of amphibolite-facies metamorphism were similar to those of the eclogite-facies formation, with fluid-induced shear zones and statically metamorphosed patches (Andersen, Austrheim, et al., 1991), and has been dated at 414 ± 2.8 Ma at conditions of 0.8–1.0 GPa and 600 °C (Glodny et al., 2002, 2008). Recent dating of amphibole-bearing pegmatite at 423 ± 1.0 Ma (Jamtveit et al., 2018) could imply that the eclogite-facies stage was shorter than previously thought.

Holsnøy is of specific interest in the Lindås nappe because eclogites are most abundant there, with only weak signs of retrogression (Austrheim, 1987; Austrheim & Griffin, 1985). Due to the very variable scale of the eclogite-facies occurrences, it is not feasible to strictly map eclogite and granulite in this area. In previous studies, ductile deformation and/or significant amounts of shear deformation are attributed to shear zones that consist of almost pure eclogite (>80%), suggesting that areas of static eclogitization are volumetrically nonsignificant (Boundy et al., 1992; Raimbourg et al., 2005).

3. Methods

We conducted field work on Holsnøy to better constrain the geometry and distribution of the eclogite-facies occurrences at various scales. We concentrate on the northwestern part of Holsnøy in order to better understand the geometries that result from partial eclogitization during deformation. The resulting map was then compiled digitally, and the height contour lines were calculated using a 10-m digital elevation model available from the geological survey of Norway (Norges Geologiske Undersøkelse, NGU). Field mapping was supported in selected areas by 3D photogrammetrical methods, using image data acquired with a DJI Phantom 4

drone from the Centre of Earth Evolution and Dynamics at the University of Oslo and the Photoscan software for processing.

Quantitative measurements of major element composition of the rock-forming minerals were obtained using a JEOL JXA 8200 SuperProbe at the Freie Universität, Berlin. Measurements were performed using an acceleration voltage of 15 kV, a beam current of 20 nA, and a beam diameter of 5 μm for feldspar and 1 μm for garnet and pyroxene. Internal calibration of the instrument was achieved using natural standards.

4. Field Relations on Holsnøy

The following will describe the petrology and structures observed during field work. Essentially the exposed rocks are granulites and eclogites (Figure 2). However, we distinguish different types using volumetric eclogite abundances as a first-order distinction, similar to previous studies (Boundy et al., 1992; Raimbourg et al., 2005). In order to better understand the differences in the rock record produced by different rock-transformation mechanisms (deformation-related or static eclogitization), structural characteristics were included as criteria for further distinction. Note that the entire region was subjected to retrogression in the amphibolite facies in varying intensities (Austrheim & Griffin, 1985; Centrella et al., 2015). As the focus of this study is the transition from granulite to eclogite, this later overprint was neglected during mapping.

4.1. The Endmembers—Granulite and Eclogite

Granulite-facies meta-anorthosites are coarse grained (1–5 mm) and in most cases have a pronounced foliation (S1) or a penetrative lineation (L1) marked by flattened or elongated coronas, respectively. These have a concentric organization, with clinopyroxene (diopside to augite) in the central part surrounded by garnet. In rare cases, the central part is composed of orthopyroxene. They are interpreted as a product of the reaction of magmatic olivine cumulates, with the surrounding plagioclase at granulite-facies conditions (Austrheim & Robins, 1981).

The granulite matrix is composed of plagioclase (typically more than ~70%), garnet, and pyroxene. Within the matrix, plagioclase is distributed homogeneously and contains zoisite needles (< 0.5 mm), usually intergrown with K-feldspar (Petley-Ragan et al., 2018), which are most abundant along grain boundaries but also occur within plagioclase grains. Plagioclase has no shape preferred orientation in thin section. Garnet aggregates are often aligned parallel to the foliation. Additional minor phases include scapolite and spinel.

Plagioclase compositions are labradoritic to andesitic (~An_{50}, Table 1). Garnet compositions are very uniform with ~$Alm_{34}Pyr_{52}Grs_{14}$ (Table 1, see also Raimbourg et al., 2007). Further, garnet grains are chemically homogeneous and have no zoning, with the exception of a 1–5 μm thick rim with higher Fe and lower Mg contents. These thin rims are generally considered to show the first onset of eclogite-facies equilibration (Raimbourg et al., 2007).

Eclogites are medium- to fine-grained (<2 mm) and mainly composed of omphacite, garnet, kyanite, and zoisite. Accessory phases include phengite, pyrite, and apatite. Some eclogites are well foliated, while others are not or only weakly foliated. The foliation is produced by the distribution and alignment of omphacite, zoisite, and kyanite that are, in well foliated eclogites, often arranged in alternating omphacite-rich and zoisite/kyanite-rich bands. In some cases, the corona structures of the protolith are preserved within the eclogite as dark deformed patches.

Garnets typically have a core consistent with the granulite-facies composition and a rim that becomes increasingly Fe-rich outward (up to Alm_{75}, Table 1). Further, garnets show healed fractures that have been sealed with a Fe-rich composition (for detailed descriptions, see Pollok et al., 2008; Raimbourg et al., 2007). Omphacite is typically unzoned, and compositions range from Jd_{38} to Jd_{42} (Table 1). Where small-scale eclogitization features are exposed, they are usually associated with evenly spaced brittle fractures, which are attributed to the volume loss during the transformation to the denser eclogite (e.g., Austrheim, 1987).

4.2. Eclogitization in Deformed Domains With Less than 50% Eclogitization

Eclogite-facies assemblages in shear zones can be observed on a wide range of scales (millimeters to hundreds of meters) on Holsnøy (Austrheim & Griffin, 1985). Brittle fractures typically cutting the granulite-facies foliation usually act as precursors for eclogitization. Their orientation seems to be unrelated to the granulite-facies fabric of the wall rock (e.g., Altenberger, 1997), and they are sometimes preserved in the center of small-scale

Tectonics

10.1029/2018TC005297

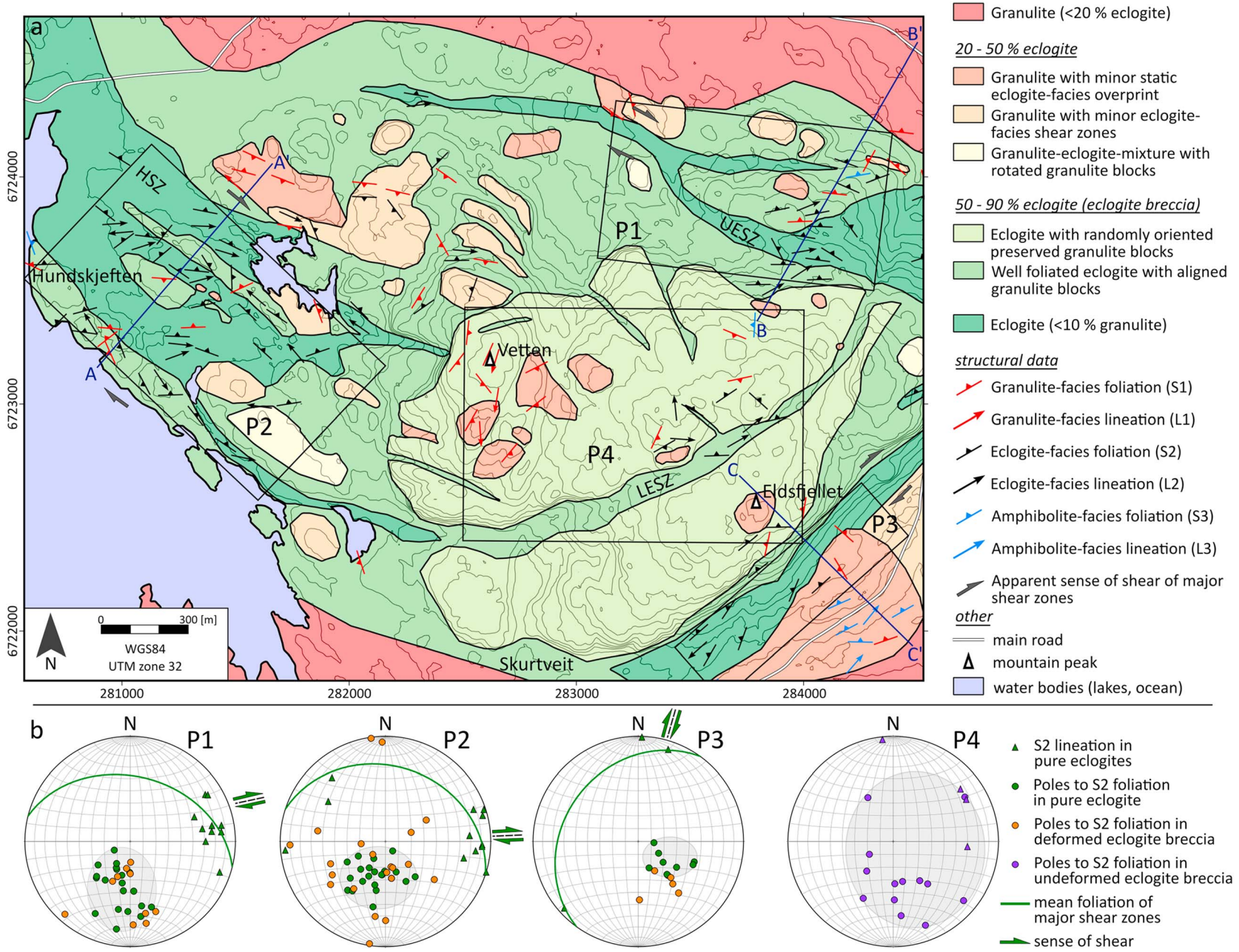

Figure 2. Geological map of the area around Eldsfjellet (NW Holsnøy). The map illustrates the distribution of the different types of eclogite and granulite occurrences that are described in the text. The amphibolite-facies overprint was omitted. The underlying height contours were calculated from a 10-m digital elevation model (available from the geological survey of Norway; Norges Geologiske Undersøkelse) and represent 20 m of elevation change. The map shows the trace of the three cross sections A, B, and C. Foliations and lineations are organized by color for granulite-facies (red), eclogite-facies (black), and amphibolite-facies (blue). The lower hemisphere equal-area projections (b) correspond to the black boxes (P1–P4). HSZ = Hundskjeften shear zone, LESZ = Lower Eldsfjellet shear zone, UESZ = Upper Eldsfjellet shear zone.

Table 1
Representative Electron Microprobe Analysis of the Major Mineral Phases of Granulites and Eclogites (in wt%)

	Garnet			Clinopyroxene			
	Granulite	Eclogite		Granulite	Eclogite		Plagioclase
SiO_2	39.82	39.21		49.01	55.34		56.30
Al_2O_3	23.09	21.77		7.33	12.56		28.63
FeO	15.86	22.42		5.82	3.32		0.05
MgO	14.56	10.22		12.49	8.27		0.00
CaO	6.03	5.63		22.38	14.77		9.18
Na_2O	—	—		1.05	5.68		4.49
K_2O	—	—		0.01	0.00		1.16
MnO	0.16	0.37		0.04	0.00		—
Cr_2O_3	0.03	0.00		0.06	0.00		—
TiO_2	0.00	0.00		1.25	0.09		—
Total	99.55	99.62		99.44	100.03		99.81
Prp	52	38	Jd	8	42	An	49
Alm	32	46	Ae	0	0	Ab	43
Sps	0	1	WEF	92	58	Or	7
Grs	16	15	XFe	0.32	0.29		

Note. that the eclogite-facies garnets typically have a granulite-facies core, consistent with the composition of granulite-facies garnets. Therefore, the measurement of the eclogite-facies garnet presented here is from the rim around a granulite-facies core. Structural formulae were calculated on the basis of 6 (clinopyroxene), 8 (plagioclase), or 12 (garnet) oxygens.

shear zones. Additionally, brittle deformation at eclogite-facies conditions is shown by the development of eclogite-facies pseudotachylytes, which might even pre-date the fracture systems that initiate fluid infiltration (e.g., Austrheim & Boundy, 1994; Bhowany et al., 2017). Further, small-scale shear zones are often accompanied by an alteration halo penetrating the surrounding granulite, which indicates the presence of fluids in the initial fracture and subsequently during ongoing eclogitization and deformation. These alteration halos are characterized by a lower degree of deformation and/or eclogitization (Figures 3a and 3b). Shear zones of this scale can typically be traced for a few meters in the granulite.

With increasing shear zone width, the eclogite-facies foliation is more pronounced, and initial precursor fractures are rarely preserved. Sets of small-scale shear zones are often parallel and, depending on their orientation, either have a dextral sense of shear (top-NE to top-SE; Figure 5), which is consistent with the regional top-E shear sense inferred for Holsnøy and the Bergen Arcs (Fossen, 1992; Raimbourg et al., 2005), or a sinistral sense of shear (top-W to top-SW; Figure 4).

When a sufficient amount of rock volume is eclogitized, the granulite blocks are increasingly isolated from each other (Figure 4). Then the orientation of the S1-foliation is disturbed because granulite blocks are rotated from their initial pre-eclogitization orientation. The eclogite forms a network of anastomosing shear zones around the rotated granulite blocks. The size of unaltered areas can vary strongly from a few centimeters to tens of meters. The width of the anastomosing shear zones increases toward the center of the shear zone network from less than 1 m to more than 10 m.

4.3. Eclogitization in Undeformed Domains With Less than 50% Eclogite

Eclogitized domains that show no signs of ductile deformation are also exposed on Holsnøy (Figures 3c and 3d). In this case eclogite-facies assemblages often, but not exclusively, develop along the granulite-facies foliation. Since the rocks in these areas have not been deformed, the granulite-facies fabric (S1-foliation) is usually preserved within the eclogite-facies assemblage (Figures 3c, 3d, 3f, and 5). Here, eclogitization advances in finger-like structures (Jamtveit et al., 2000), often originating from fractures, which are generally oblique to the granulite-facies foliation, similar to the shear zones described above. In some cases, a small offset (<10 cm) can be observed along the initial fracture (Figure 5). The size of these statically eclogitized patches can reach more than 5 m in diameter. The transition from the granulite into the eclogite is not sharp, as shown by a progressive increase in the amount of omphacite. Within the transition between granulite and eclogite, both omphacite and plagioclase are present, implying a kinetic limiting factor of the eclogitization process (Austrheim, 1987).

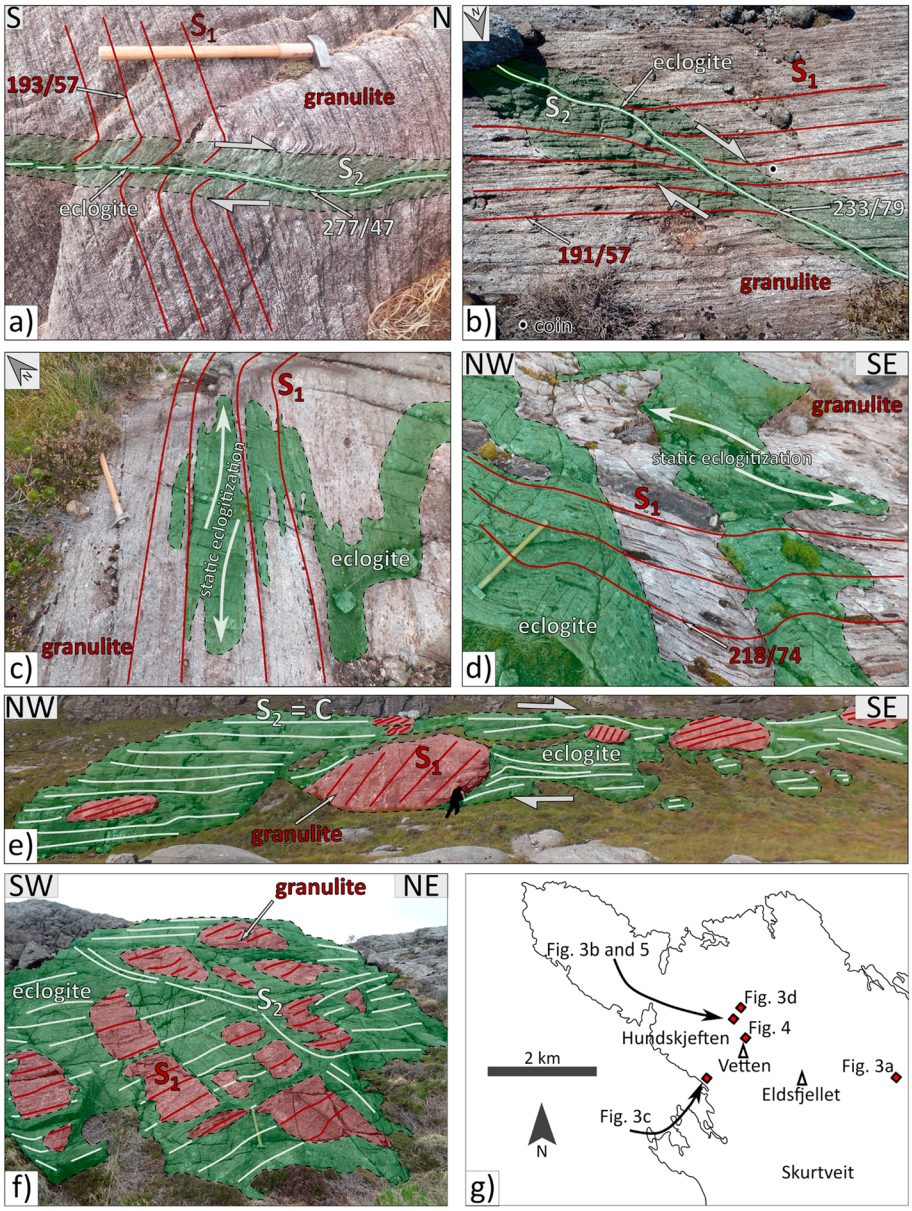

Figure 3. Photographs of typical small-scale shear zones (a, b) and static eclogitization patches (c, d) on Holsnøy. Typical outcrops of eclogite breccia are shown in (e) (sheared eclogite breccia) and (f) (unsheared eclogite breccia). Note that the central part of (f) is cut by a small shear zone, which deforms the granulite block next to it (adjacent to S2 label). Granulites are shown in red and eclogites in green. The trend of the granulite foliation (S1) is also shown in red while the trend of the eclogite foliation (S2) is shown in white. In (a) and (b), the shear zones are divided into three parts: dark green = eclogitized and deformed shear zone center, light green = transitional zone into the pristine granulite (red). A scale is provided as a hammer (a, c, d, and f), a coin (b), or a person (e). Measurements of the eclogite and granulite foliation are provided in red (granulite) and white (eclogite). Since the foliation is mostly unaffected by the change in lithology for the static type (c, d), it is shown as the granulite foliation (red). (g) The locations of (a–f) and Figures 4 and 5.

These static eclogitization patterns can coexist in the same outcrop with the small-scale eclogite-facies shear zones described above. Additionally, both static as well as deformation-related (dynamic) eclogitization structures can exist isolated from each other.

4.4. Eclogitization in Domains With 50–90% Eclogitization (*Eclogite Breccia*)

The eclogite breccia (Boundy et al., 1992) can be subdivided into two main types using structural observations: a highly sheared type and a nonsheared type (Figures 3e and 3f). The volumetric abundance of

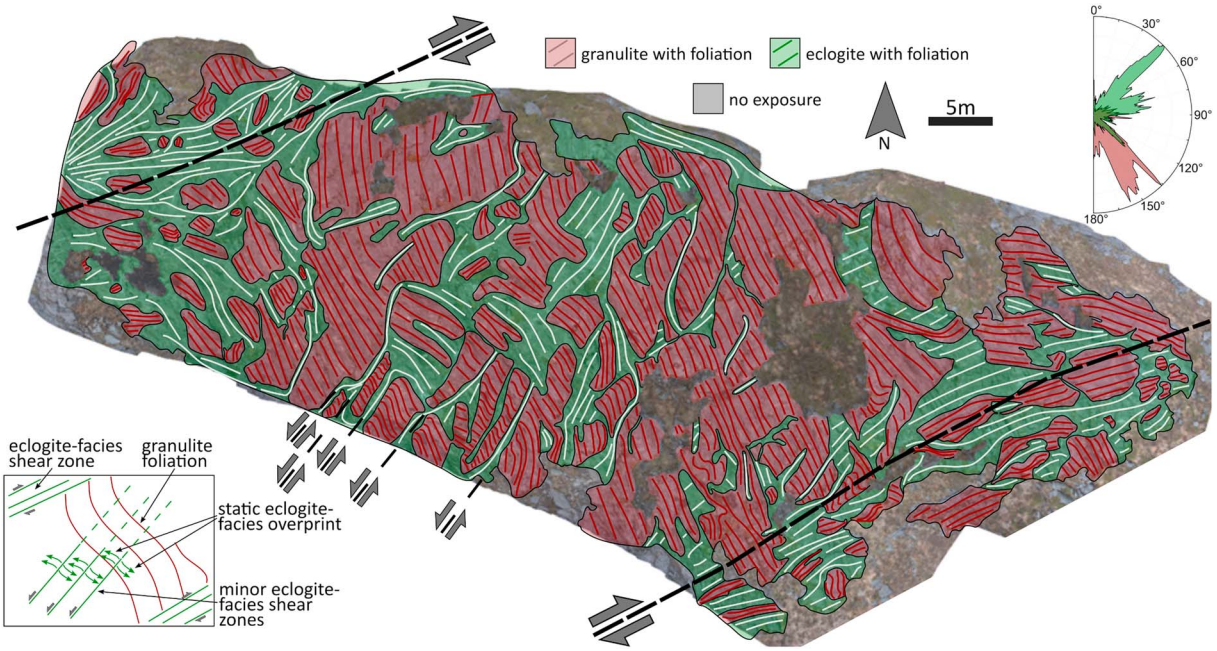

Figure 4. Interpretation of an outcrop using three-dimensional photogrammetry from 157 drone images. It shows granulite in red and eclogite in green including the trend of the foliation for eclogite (white) and granulite (red). The central part shows sinistral shear zones trending NE-SW and patches of static eclogite-facies overprint (foliation trending NW-SE). The upper left and lower right parts show how the preserved granulite blocks are integrated into larger shear zones. The inset shows a simplified illustration of the changing foliation trend. In the upper right, a normalized rose diagram shows the trend of the both the eclogite and the granulite foliation.

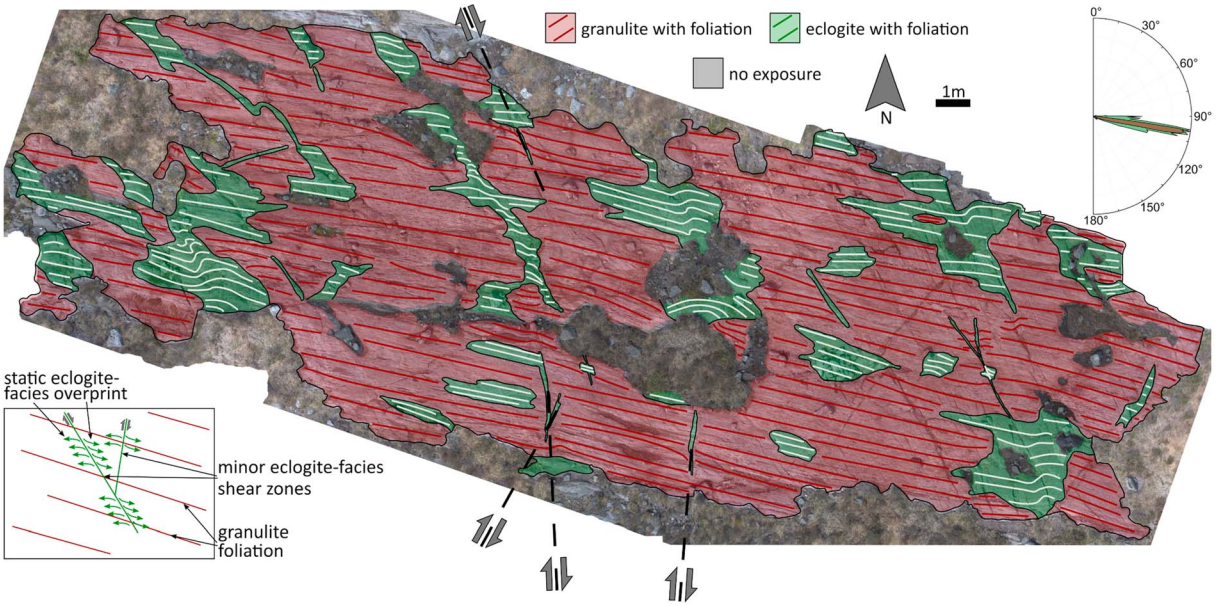

Figure 5. Interpretation of an outcrop showing eclogite in green and granulite in red. The image was generated using three-dimensional photogrammetry compiled from 112 drone images. The granulite is cut by two conjugated sets of thin shear zones from which static eclogitization consumes the granulite along its foliation. The eclogite foliation is shown in white and the granulite foliation in red. The inset (lower left) shows a simplified illustration of the general structure of the same outcrop, and the normalized rose diagram (upper right) shows the general trend of the eclogite and granulite foliations.

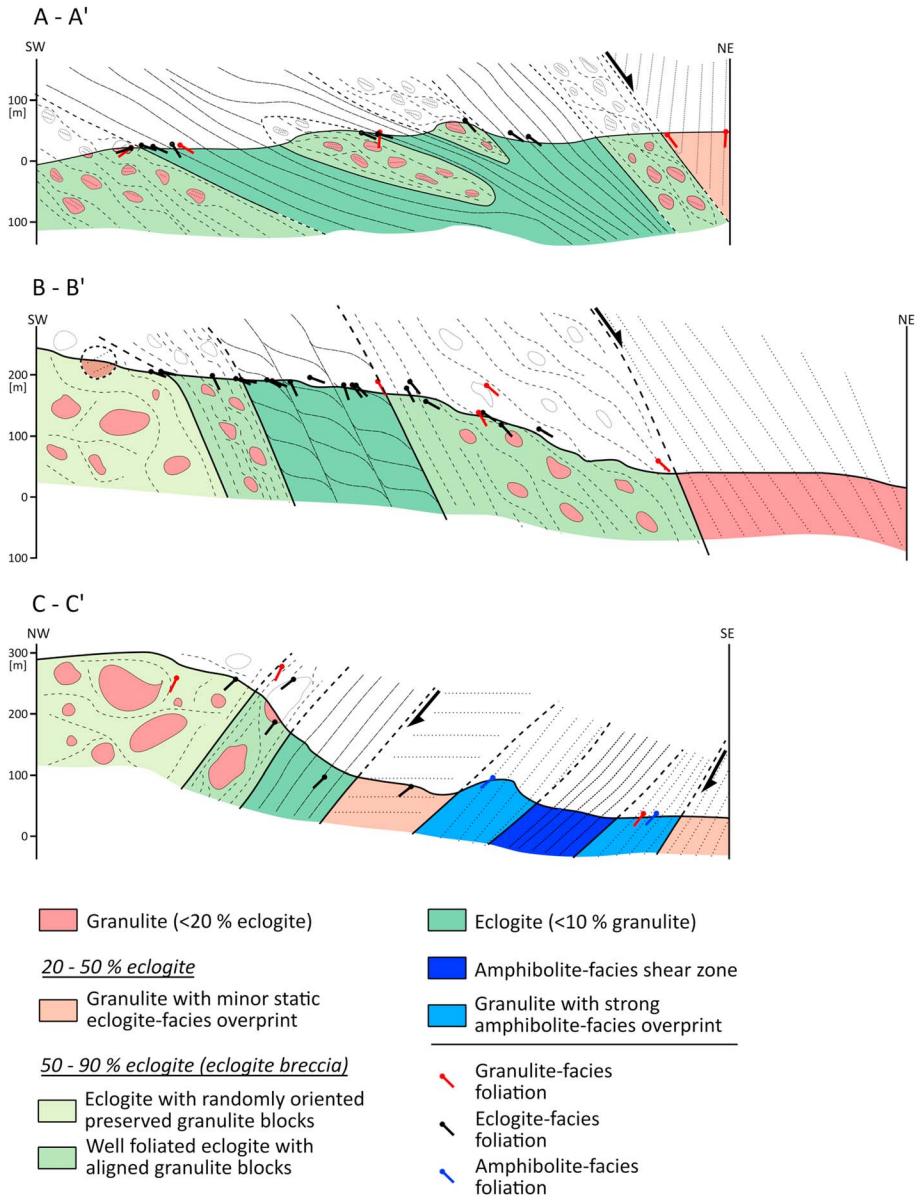

Figure 6. Cross sections of three major shear zones: A-A′ = Hundskjeften shear zone, B-B′ = Upper Eldsfjellet shear zone, and C-C′ = Skurtveit shear zone. The trace of the three cross sections is indicated in Figure 2. The preserved granulite blocks shown in all three cross sections are exaggerated in size (in the field they range from a few centimeters to ~100 m) but illustrate the approximate size relationships to each other. The orientation of the foliation was projected onto the trace of the cross section and is shown for eclogite-facies (green), granulite-facies (red), and amphibolite-facies (blue).

eclogite is the same for both types (50–90%). The sheared eclogite breccia has a pronounced eclogite-facies foliation, which wraps around isolated granulite blocks ranging in size from a few centimeters to ~10 m (Figure 3e). The longer axis of these blocks is oriented parallel or subparallel to the eclogite-facies foliation (S2) and the shear plane, respectively. Additionally, the long axis of the blocks is often also parallel or subparallel to the trend of the granulite-facies foliation preserved within the granulite blocks (Figure 3e). The transition from preserved granulite blocks to eclogite matrix is typically sharp. The sheared eclogite breccia can reach a thickness of up to a few hundred meters and lengths of 1–2 km and typically has the same sense of shear as the main shear zone that it surrounds (Figure 6).

The eclogite breccia that is mostly unaffected by ductile deformation (in the following termed unsheared eclogite breccia) is only weakly foliated or in rare cases not foliated at all. If a foliation is present, it is

usually very variable in its orientation. Additionally, the shape of the preserved granulite blocks is irregular (Figure 3f), and the granulite-facies foliation, preserved within granulite blocks, has no constant or preferred orientation. The borders of granulite blocks are diffuse. Areas dominated by unsheared eclogite breccia can be up to a few hundred meters across. Unsheared eclogite breccia can show some offset in localized areas, but a consistent sense of shear cannot be identified for more than a few meters.

Both types of eclogite breccia can contain larger blocks (>100 m) that are internally structured. These usually have small-scale eclogitization structures that are either static or deformed (as described above), or a mixture of the two. Blocks of this type were included in the map (e.g., Hundskjeften area in Figure 2) when their dimensions were sufficient to be distinguished on the map scale.

4.5. Major Shear Zones

Although shear zones of all sizes, from the centimeter to the kilometer scale, occur on Holsnøy, four major eclogite-facies shear zones can be distinguished in map view (Figures 2 and 6). These were described by previous authors (e.g., Boundy et al., 1997; Fountain et al., 1994; Raimbourg et al., 2005): (1) the Hundskjeften shear zone (HSZ; Figure 6a), (2) the Upper Eldsfjellet shear zone (UESZ; Figure 6b), (3) the Lower Eldsfjellet shear zone (LESZ), and (4) the Skurtveit shear zone (SSZ; Figure 6c). The HSZ and UESZ trend NW-SE and have a top-ENE sense of shear and the SSZ and the LESZ trend SW-NE and have a top-NNE sense of shear.

In previous studies, these major shear zones have been considered to be limited to the areas of almost complete eclogitization (>80%; Boundy et al., 1992; Raimbourg et al., 2005). However, areas with a significant amount of preserved granulite blocks need to be included when investigating the main shear zone structure. Figure 6 shows cross sections constructed across three of the four major shear zones (see Figure 2 for the locations of the transects). In all three cases, the zone of maximum eclogitization (>90%) is bounded by zones where well-ordered granulite blocks are contained within the eclogite matrix, that is, the sheared eclogite breccia (Figures 3e and 6), representing a transitional zone away from the main shear zone. In sections A and B, these zones occur on both sides of the shear zone, while in section C only one side is bounded by eclogite breccia (Figure 6).

The thickness of the major shear zones varies from approximately 220 (section C) up to 730 m (section B), when including the sheared eclogite breccia as part of the shear zone. The minimum thickness of the HSZ (section A) is approximately 410 m (Figure 6). The HSZ, however, is not exposed in its entire thickness (Figures 2 and 6). In sections A and C, the thickness of the eclogite breccia accounts for approximately 40% of the entire shear zone thickness, while 70% of the shear zone thickness in section B is attributed to the sheared eclogite breccia.

Foliation and lineation measurements show that the HSZ and the UESZ have a top-ENE sense of shear, while the SSZ has a top-NNE sense of shear (Figure 2b). Additionally, the comparison of measurements from the shear zone center (almost entirely converted to eclogite) to the measurements from the surrounding eclogite breccia shows that the foliation in the shear zone center is less variable, likely due to stronger deformation (Figure 2b).

5. Discussion

The structures observed on Holsnøy have been studied extensively (e.g., Austrheim, 1987; Austrheim & Griffin, 1985; Bhowany et al., 2017; Bjørnerud & Austrheim, 2004; Boundy et al., 1992; Camacho et al., 2005; Cohen et al., 1988; Griffin, 1972; Jamtveit et al., 1990; Jamtveit, Ben-Zion, et al., 2018; Jolivet et al., 2005; Raimbourg et al., 2005). A general consensus is that the complex exposed on Holsnøy constitutes an excellent example of dry granulite-facies lower continental crust, where the deformation and eclogitization processes during HP-LT metamorphism in a continental collision or subduction setting can be studied at the surface (e.g., Jackson et al., 2004; Jolivet et al., 2005; Putnis et al., 2017). In that sense, previous studies have concluded that the main factor controlling how the subducting crust is being altered is deformation associated with fluid infiltration (Austrheim, 1987), leaving large areas of the crust unaltered during subduction when there is no fluid present. Regarding this, it has to be noted that the area of Holsnøy where extensive eclogitization is preserved is small when compared to the remainder of the Lindås nappe, where there are only few reports of eclogite occurrences (Figure 1). The southeastern part of Holsnøy is also devoid of any signs of mineral reactions at eclogite-facies conditions (e.g., Schmid et al., 1998). However, the remainder

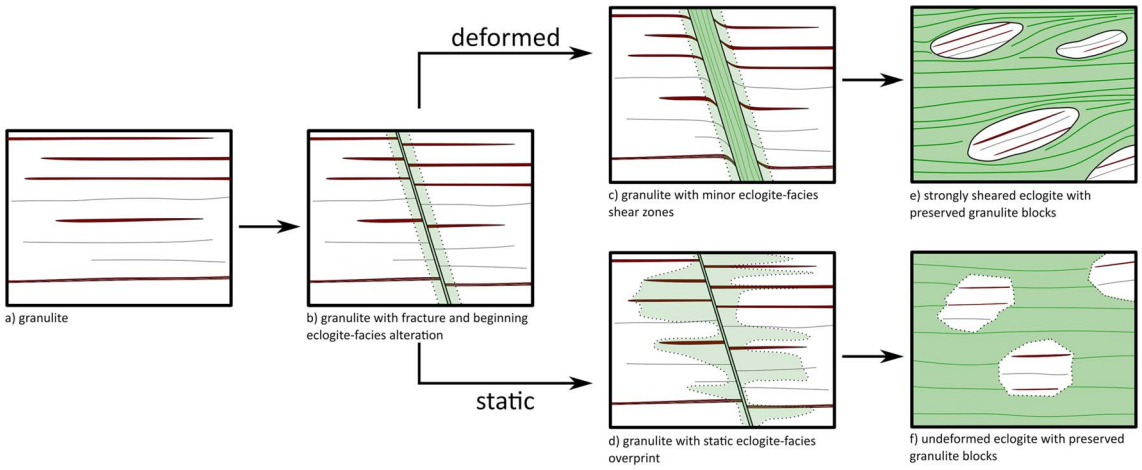

Figure 7. Schematic representation depicting the evolution of eclogite occurrences as exposed on Holsnøy. The different sketches (a–f) correspond to the eclogite-facies structures described in the text. (a) Pristine granulite; (b) beginning eclogitization of the granulite through a precursor fracture that was infiltrated by fluids. The light green zone represents the reaction halo. (c) Granulite with a minor eclogite-facies shear zone, (d) sketch showing how the eclogite-facies overprint (light green) progresses parallel to the granulite-facies foliation without any deformation, (e) sheared eclogite breccia, and (f) unsheared eclogite breccia. (c, (e) The deformed path of eclogitization and (d, f) the undeformed path. Details are described in the text.

of the Lindås nappe must have been at the same or at least similar *P-T* conditions during the Caledonian collision as the extensively eclogitized area on Holsnøy (Putnis et al., 2017).

5.1. Static Versus Deformation-Related Eclogitization

According to previous studies (e.g., Austrheim, 1987; Boundy et al., 1992; Jamtveit, Moulas, et al., 2018; Raimbourg et al., 2005), there is a strong link between fluid availability, deformation, and eclogite-facies metamorphism. This, however, does not apply to large areas where a high degree of eclogitization occurs in the absence of significant or pervasive ductile deformation. In order to understand the interplay between static eclogitization and eclogitization with associated deformation, these two end-members have to be examined separately (Figure 7).

As previous studies have shown the deformation-controlled case is initiated by brittle fractures (e.g., Austrheim, 1987). Eclogite-facies pseudotachylytes in the area indicate that the granulites behave in a brittle manner even at eclogite-facies *P-T* conditions (Austrheim & Boundy, 1994; Austrheim et al., 1996, 2017; Jamtveit, Ben-Zion, et al., 2018). This is supported by fracturing and subsequent healing of granulite-facies garnets (Pollok et al., 2008; Raimbourg et al., 2007). Fluid infiltration then occurs along brittle fractures that open the necessary fluid pathways and cause the previously metastable granulite to transform into eclogite (Austrheim, 1987). Sets of shear zones, depending on their orientation, are either dextral (top-NE to top-SE) consistent with the contractional sense of shear of the Bergen Arcs (Fossen, 1992; Raimbourg et al., 2005) or sinistral (top-W to top-SW) in which case they indicate bookshelf-style faulting (Raimbourg et al., 2005). During ongoing deformation, the continuing propagation and widening of shear zones causes the formation of shear zone networks and eventually the integration of these networks into larger-scale shear zones (Jolivet et al., 2005), some of which still contain significant amounts of preserved granulite blocks (Figures 2, 4, and 6; Boundy et al., 1992).

However, many of the eclogitization features presented here cannot be explained by this classical sequence. On the outcrop-scale, eclogitization often occurs parallel to the granulite-facies foliation without associated ductile deformation (Figure 5). While the necessary fluid here is also initially introduced into the granulite by brittle fractures, these zones do not undergo significant deformation during advancement of the fluid-mediated reaction front into the wall rock (Figures 5 and 7d). Nevertheless, the granulite-facies mineral assemblage is replaced by an eclogite-facies mineral assemblage without any indication of associated penetrative ductile deformation (static eclogitization; Figures 3f and 7f). Due to the low permeability of the granulite, this is best explained by transient porosity phenomena produced by dissolution-precipitation reactions (Plümper et al., 2017).

While previous studies on Holsnøy have described static eclogitization at the outcrop scale (Jamtveit et al., 2000), the process has not been given any significance on a larger scale. However, in some areas the eclogite breccia exhibits features that are not compatible with pervasive ductile deformation during eclogitization. Adjacent to major shear zones, the eclogite breccia is well foliated, and the preserved granulite blocks are typically aligned with their long axis more or less parallel to the eclogite-facies foliation (Figure 3e); that is, they have rotated into a stable position, as is expected during shearing (e.g., Fossen & Cavalcante, 2017; Jeffery, 1922). In the unsheared eclogite breccia, however, the preserved granulite blocks are almost randomly oriented, with respect to their aspect ratio, and if the eclogite exhibits a newly formed foliation (Figure 3f), it is significantly less evolved than in the sheared eclogite breccia. This indicates that the processes active during formation of the sheared eclogite breccia are significantly different from those active during formation of the unsheared eclogite breccia. Those parts of the eclogite breccia with randomly oriented granulite blocks and weak eclogite-facies foliation cannot have undergone pervasive ductile deformation. Nevertheless, in these areas eclogites are volumetrically similarly abundant as in the sheared eclogite breccia, suggesting a significant influence of static eclogitization on a regional scale.

This means that during ongoing deformation and fluid infiltration and shear zone network formation (Figures 7b and 7c), areas affected by static eclogitization grow in size, as well. It seems clear that fluid migration during shear zone growth is controlled by the ongoing ductile deformation (e.g., Fusseis et al., 2009). However, due to the low porosity of the granulite, it is more difficult to understand the fluid migration pathways in the static case. Jamtveit et al. (1990) proposed that the density increase and thus volume decrease due to the eclogitization reaction might have enhanced permeability for fluid transport. Additionally, studies have shown that in a rock with low permeability, mineral reactions produce transient porosities and thus generate fluid pathways (Plümper et al., 2017).

Because the rock softens when it is infiltrated by fluids and while undergoing metamorphic reactions, zones of static eclogitization are prone to experience minor differential movement between adjacent rigid blocks (i.e., the unaltered granulite). Hence, they can exhibit very small-scale shear zones diffusely deformed with inconsistent kinematics. However, this deformational overprint is significantly different (Figures 3e, 3f, 7e, and 3f) from the classic eclogite-facies shear zones that are observed on Holsnøy because, due to the lack of significant deformation, no consistent shear sense can be established in these domains.

On Holsnøy, all of the described structures are well exposed (Figure 2). The mountainous Eldsfjellet area constitutes a large block-like body of mostly unsheared eclogite breccia (Figure 2). It is surrounded by the major eclogite-facies shear zones: the UESZ to the north, the SSZ to the east, and the HSZ to the south. It therefore represents a domain that was not significantly affected by the ductile deformation that shaped this part of the Lindås nappe (i.e., a low-strain domain). Thus, it is considered to be a block with a diameter of ~2 km within a highly strained matrix. From the map view (Figure 2) alone, the different behavior during ongoing deformation can be discerned. Shear zones are elongated or tabular structures that accumulate strain (Fossen & Cavalcante, 2017), while the shape of the Eldjfellet area is more or less round and characterized by low-strain accumulation, as is also supported by the irregular or almost random orientation of the eclogite-facies foliation (P4 in Figure 2b). In contrast, the foliation in the surrounding major shear zones is well defined and regularly oriented (P1 to P3 in Figure 2b). Additionally, lineation measurements in the Eldsfjellet area, although there are few, indicate stretching in various directions (P4 in Figure 2b), while the orientation of the lineation from the surrounding shear zones is internally consistent, that is, E-W to ENE-WSW in the HSZ and UESZ and ~NE–SW in the SSZ.

The sense of shear of the major shear zones surrounding the low-strain domain is consistent (top-E to top-NE; Figure 2). They wrap around the low-strain domain, similar to how the foliation in the sheared eclogite breccia wraps around preserved granulite blocks (Figures 2 and 6). The low-strain domain can be thus interpreted as a large block within a matrix similar to a sigma-clast (Passchier & Simpson, 1986) that gives a top-ESE sense of shear (Figure 2), which is generally consistent with top-E directed Caledonian shortening in the Bergen Arcs (Fossen, 1992; Raimbourg et al., 2005).

The map presented here (Figure 2) also implies that while most of the strain localizes within the almost completely eclogitized zones, a significant amount is also distributed in the sheared eclogite breccia that can constitute up to 70% of the total shear zone thickness (Figure 6). The foliation measurements in Figure 2 show

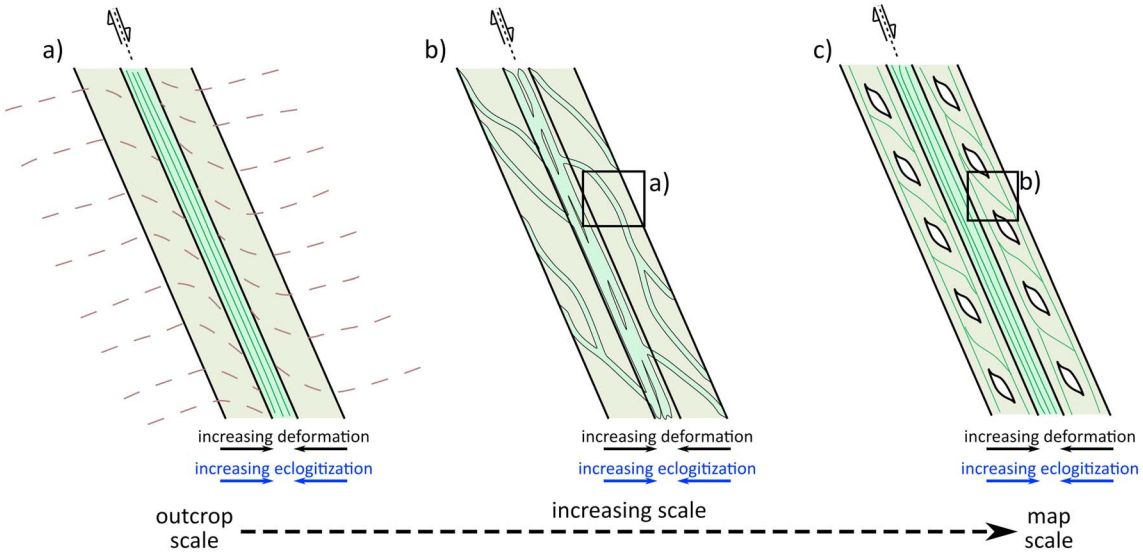

Figure 8. Schematic illustration of the general shear zone geometries on different scales: (a) outcrop scale showing the general setup of strong deformation and eclogitization in the central part (darker green) and the transitional (light green) degree of eclogitization and deformation outward into the unaltered granulite (light red). Red and green lines show the granulite- and eclogite-facies foliations, respectively. (b) Intermediate scale showing how the single small-scale shear zones (a) form shear zone networks. Here there is typically a central part with many and wider shear zones and a transitional zone with fewer and less pronounced shear zones (light green) until only the unaltered granulite remains. (c) Typical schematic illustration of the map-scale shear zones with the completely eclogitized and strongly deformed shear zone in the center bounded by eclogite breccia.

that the eclogite breccia is not as well ordered in terms of consistency of the foliation as the localized zones in the shear zone center.

These observations imply that the significance of static eclogitization on Holsnøy has been underestimated in the past. Large areas of Holsnøy have been subjected to static re-equilibration in the eclogite-facies without exhibiting significant deformation (low-strain domains; Figure 2). When considering Holsnøy as an analogue for partial eclogitization of a subducting metastable crust (Austrheim, 1987; Jackson et al., 2004; Putnis et al., 2017), this puts a new perspective on the interplay between deformation and metamorphism during subduction. That large crustal areas can remain unreacted during subduction or deep burial in a collisional setting if they remain dry has been established by several authors in the past (e.g., Andersen et al., 1991; Austrheim, 1987, 2013; Bjørnerud et al., 2002; Jamtveit et al., 1990; John & Schenk, 2003). However, fluid infiltration with associated ductile deformation was previously identified as the main driving factor. While this remains an important and very efficient process to transform crustal rocks to eclogites, the effect of a static eclogite-facies overprint needs to be considered.

5.2. Scale Dependence of the Structural Framework

The area of Holsnøy and the structural framework it exposes have been widely used to study and illustrate how dry crustal rocks are deformed and eclogitized during deep burial. A well-established sequence of how deformation progresses from centimeter-scale shear zones to shear zones with thicknesses of a few hundred meters can be observed from outcrop to map scale. With this time-dependent sequence being established, it poses the question of how the general structural framework varies over different spatial scales.

In the case of Holsnøy, it is evident that single small-scale shear zones combine into networks before they form map-scale shear zones with a thickness of up to a few hundred meters (e.g., Austrheim, 1987; Jolivet et al., 2005). Figure 8 illustrates this in three simplified sketches (Figures 8a–8c).

This sequence begins with a single small-scale shear zone (Figure 8a). As shown in Figure 3, this shear zone has an eclogitized and sheared central part, while the outer parts are transitional into the undeformed granulite, both with respect to the degree of deformation as well as the degree of eclogitization. With progressive deformation and eclogitization, such shear zones begin to form networks (Figure 8b), which typically have a central part with many relatively wide shear zones and few granulite remnants

in between. The outer part consists of fewer and less evolved shear zones gradually transitioning into the undeformed granulite. The geometry of single shear zones in this outer part is an analogue to the single shear zone in Figure 8a. The general geometry of the map-scale shear zones (Figures 2 and 6) is illustrated in Figure 8c. As described before, these (central part Figure 8c) are typically bounded on both sides by the sheared eclogite breccia (Figures 2 and 6) that serves as the transition from the shear zone into the undeformed granulite.

Independent of the observed scale, both eclogitization and deformation are most intense in the shear zone center and gradually decrease outward, suggesting that the general geometry in a qualitative sense is scale-independent. While this observation seems trivial for a ductile shear zone (e.g., Fossen & Cavalcante, 2017), the validity of this relationship from the meter scale to the kilometer scale and across a hierarchy of deformation structures (spanning several orders of magnitude) has significant implications for the understanding of the structures exposed on Holsnøy.

In addition, preserved granulite blocks within the eclogite breccia (sheared and unsheared) essentially constitute the same structural framework as Holsnøy in its entirety. Across scales (outcrop scale, cross sections, or map scale), low-strain domains surrounded by eclogite-facies shear zones are present.

The scale-invariance of the structures implies that crustal-scale shear zones in a collision setting can be expected to develop similar geometric configurations. For example, the East Tenda Shear Zone (Corsica, France), which is the result of alpine deformation of mid- to upper crustal rocks, has very similar features. Here blueschist-facies shear zones cut crustal rocks in networks that surround low-strain domains consisting of mostly undeformed and metastable granitoids (Maggi et al., 2012). While heterogeneous deformation in itself is not a surprising feature (e.g., Fossen & Cavalcante, 2017), these observations on Holsnøy underline the relevance of the geometry for deformation and metamorphism during subduction and collision. This suggests that crustal-scale shear zones truncating crystalline rocks in active subduction and collision settings likely have a similar general geometry.

In addition, the scale invariance has important implications for seismological studies in currently active settings. The structures described here, including the map-scale features, are far below the wavelength typically used for seismological studies. For example, in high-resolution receiver function studies, periods of less than 1 s are rarely usable, resulting in a wavelength for *S* waves of ~4 km. Additionally, the horizontal resolution will be further limited by the Fresnel condition. Hence, such structures will contribute to the bulk properties as an effective medium (Mavko et al., 2009). Because of the scale invariance, observations at one scale can be used as exemplary cases to bridge the scales, at least in a qualitative sense.

6. Conclusions

The results presented here largely confirm the link between eclogitization and deformation identified by previous studies, leading to the concept of dynamic eclogitization. However, we show that static eclogitization, that is, eclogitization without associated deformation, is also an important process. Based on our new detailed map of Holsnøy, which unlike most previous maps distinguishes the relative amount of strain under eclogite-facies conditions independently from the degree of eclogitization, we conclude that the interplay between static and dynamic eclogitization, and which of these two is dominant at one point in space and/or time, produces distinctly different structural results over a range of scales. It shows that static eclogitization is not limited to small patches on Holsnøy but affected large areas of the subducting lower crust. Subsequently, some of these areas were affected by minor amounts of deformation partially masking the static eclogitization signature but are still clearly distinguishable from the map-scale shear zones because preserved granulite blocks are not ordered or aligned systematically and no consistent penetrative foliation is present. This clearly shows that large low-strain domains can be preserved within deeply buried material even during ongoing intense deformation in the same area. The possibility of such structures in currently active subduction zones has a direct effect on their interpretation (e.g., seismological studies) as, for example, the expected seismic anisotropy would be reduced in areas of static transformation.

Further, the observed geometries have significant similarities across different scales. Although this has previously been shown for other shear zone networks (e.g., Fossen & Cavalcante, 2017; Schrank et al., 2008),

Holsnøy stands out for preserving a kilometer-scale lower crustal shear zone network, which was not significantly modified during exhumation and exhibits self-similarity across several orders of magnitude. This self-similarity illustrates the relevance of the general structural framework of Holsnøy for processes such as subduction, indicating that crustal-scale shear zones in currently active settings likely form the same geometric configurations.

Acknowledgments
We thank Hans Jørgen Kjøll from the Centre for Earth Evolution and Dynamics (Oslo, Norway) for help with acquiring drone images (funded by research grant 250327/F20 from the Research Council of Norway) during field work. This research was supported by the Deutsche Forschungsgemeinschaft (DFG) in the framework of the priority program SPP 2017 "Mountain Building Processes in Four Dimensions (MB-4D)" by grant JO 349/11-1. The authors thank John Geissman for editorial handling and Uwe Altenberger and one anonymous reviewer for their suggestions that significantly improved the manuscript. All additional data used in this manuscript can be found in the supporting information.

References

Altenberger, U. (1997). Strain localization mechanisms in deep-seated layered rocks. *Geologische Rundschau*, *86*(1), 56–68. https://doi.org/10.1007/s005310050121

Altenberger, U., & Wilhelm, S. (2000). Ductile deformation of K-feldspar in dry eclogite facies shear zones in the Bergen Arcs, Norway. *Tectonophysics*, *320*(2), 107–121. https://doi.org/10.1016/S0040-1951(00)00048-2

Andersen, T., Austrheim, H., & Burke, E. A. J. (1990). Fluid inclusions in granulites and eclogites from the Bergen Arcs, Caledonides of W. Norway. *Mineralogical Magazine*, *54*(375), 145–158. https://doi.org/10.1180/minmag.1990.054.375.02

Andersen, T., Austrheim, H., & Burke, E. A. J. (1991). Fluid-induced retrogression of granulites in the Bergen Arcs, Caledonides of W. Norway: Fluid inclusion evidence from amphibolite-facies shear zones. *Lithos*, *27*(1), 29–42. https://doi.org/10.1016/0024-4937(91)90018-G

Andersen, T. B., Berry, H. N., Lux, D. R., & Andresen, A. (1998). The tectonic significance of pre-Scandian $^{40}Ar/^{39}Ar$ phengite cooling ages in the Caledonides of western Norway. *Journal of the Geological Society*, *155*(2), 297–309. https://doi.org/10.1144/gsjgs.155.2.0297

Andersen, T. B., Corfu, F., Labrousse, L., & Osmundsen, P.-T. (2012). Evidence for hyperextension along the pre-Caledonian margin of Baltica. *Journal of the Geological Society*, *169*(5), 601–612. https://doi.org/10.1144/0016-76492012-011

Andersen, T. B., Jamtveit, B., Dewey, J. F., & Swensson, E. (1991). Subduction and eduction of continental crust: Major mechanisms during continent-continent collision and orogenic extensional collapse, a model based on the south Norwegian Caledonides. *Terra Nova*, *3*(3), 303–310. https://doi.org/10.1111/j.1365-3121.1991.tb00148.x

Austrheim, H. (1987). Eclogitization of lower crustal granulites by fluid migration through shear zones. *Earth and Planetary Science Letters*, *81*(2-3), 221–232. https://doi.org/10.1016/0012-821X(87)90158-0

Austrheim, H. (1990). The granulite-eclogite facies transition: A comparison of experimental work and a natural occurrence in the Bergen Arcs, western Norway. *Lithos*, *25*(1-3), 163–169. https://doi.org/10.1016/0024-4937(90)90012-P

Austrheim, H. (2013). Fluid and deformation induced metamorphic processes around Moho beneath continent collision zones: Examples from the exposed root zone of the Caledonian mountain belt, W-Norway. *Tectonophysics*, *609*, 620–635. https://doi.org/10.1016/j.tecto.2013.08.030

Austrheim, H., & Boundy, T. M. (1994). Pseudotachylytes generated during seismic faulting and eclogitization of the deep crust. *Science*, *265*(5168), 82–83. https://doi.org/10.1126/science.265.5168.82

Austrheim, H., Dunkel, K. G., Plümper, O., Ildefonse, B., Liu, Y., & Jamtveit, B. (2017). Fragmentation of wall rock garnets during deep crustal earthquakes. *Science Advances*, *3*, 1–8. https://doi.org/10.1126/sciadv.1602067

Austrheim, H., Erambert, M., & Boundy, T. M. (1996). Garnets recording deep crustal earthquakes. *Earth and Planetary Science Letters*, *139*(1-2), 223–238. https://doi.org/10.1016/0012-821X(95)00232-2

Austrheim, H., & Griffin, W. L. (1985). Shear deformation and eclogite formation within granulite-facies anorthosites of the Bergen Arcs, western Norway. *Chemical Geology*, *50*(1-3), 267–281. https://doi.org/10.1016/0009-2541(85)90124-X

Austrheim, H., & Robins, B. (1981). Reactions involving hydration of orthopyroxene in anorthosite-gabbro. *Lithos*, *14*(4), 275–281. https://doi.org/10.1016/0024-4937(81)90055-4

Bascou, J., Barruol, G., Vauchez, A., Mainprice, D., & Egydio-Silva, M. (2001). EBSD-measured lattice-preferred orientations and seismic properties of eclogites. *Tectonophysics*, *342*(1-2), 61–80. https://doi.org/10.1016/S0040-1951(01)00156-1

Bhowany, K., Hand, M., Clark, C., Kelsey, D. E., Reddy, S. M., Pearce, M. A., et al. (2017). Phase equilibria modelling constraints on P–T conditions during fluid catalysed conversion of granulite to eclogite in the Bergen Arcs, Norway. *Journal of Metamorphic Geology*, *36*(3), 315–342. https://doi.org/10.1111/jmg.12294

Bingen, B., Austrheim, H., Whitehouse, M. J., & Davis, W. J. (2004). Trace element signature and U–Pb geochronology of eclogite-facies zircon, Bergen Arcs, Caledonides of W Norway. *Contributions to Mineralogy and Petrology*, *147*(6), 671–683. https://doi.org/10.1007/s00410-004-0585-z

Bingen, B., Davis, W. J., & Austrheim, H. (2001). Zircon U-Pb geochronology in the Bergen arc eclogites and their Proterozoic protoliths, and implications for the pre-Scandian evolution of the Caledonides in western Norway. *Geological Society of America Bulletin*, *113*(5), 640–649.

Bjørnerud, M. G., & Austrheim, H. (2004). Inhibited eclogite formation: The key to the rapid growth of strong and buoyant Archean continental crust. *Geology*, *32*(9), 765–768. https://doi.org/10.1130/G20590.1

Bjørnerud, M. G., Austrheim, H., & Lund, M. G. (2002). Processes leading to eclogitization (densification) of subducted and tectonically buried crust. *Journal of Geophysical Research*, *107*(B10), 2252. https://doi.org/10.1029/2001JB000527

Bostock, M., Hyndman, R., Rondenay, S., & Peacock, S. (2002). An inverted continental Moho and serpentinization of the forearc mantle. *Nature*, *417*(6888), 536–538. https://doi.org/10.1038/417536a

Boundy, T. M., Donohue, C. L., Essene, E. J., Mezger, K., & Austrheim, H. (2002). Discovery of eclogite facies carbonate rocks from the Lindås Nappe, Caledonides, Western Norway. *Journal of Metamorphic Geology*, *20*(7), 649–667. https://doi.org/10.1046/j.1525-1314.2002.00396.x

Boundy, T. M., Fountain, D. M., & Austrheim, H. (1992). Structural development and petrofabrics of eclogite facies shear zones, Bergen Arcs, western Norway: Implications for deep crustal deformational processes. *Journal of Metamorphic Geology*, *10*(2), 127–146. https://doi.org/10.1111/j.1525-1314.1992.tb00075.x

Boundy, T. M., Mezger, K., & Essene, E. J. (1997). Temporal and tectonic evolution of the granulite-eclogite association from the Bergen Arcs, western Norway. *Lithos*, *39*(3-4), 159–178. https://doi.org/10.1016/S0024-4937(96)00026-6

Camacho, A., Lee, J. K. W., Hensen, B. J., & Braun, J. (2005). Short-lived orogenic cycles and the eclogitization of cold crust by spasmodic hot fluids. *Nature*, *435*(7046), 1191–1196. https://doi.org/10.1038/nature03643

Centrella, S., Austrheim, H., & Putnis, A. (2015). Coupled mass transfer through a fluid phase and volume preservation during the hydration of granulite: An example from the Bergen Arcs, Norway. *Lithos*, *236-237*, 245–255. https://doi.org/10.1016/j.lithos.2015.09.010

Cohen, A. S., O'Nions, R. K., Siegenthaler, R., & Griffin, W. L. (1988). Chronology of the pressure-temperature history recorded by a granulite terrain. *Contributions to Mineralogy and Petrology*, *98*(3), 303–311. https://doi.org/10.1007/BF00375181

Corfu, F., Andersen, T. B., & Gasser, D. (2014). The Scandinavian Caledonides: Main features, conceptual advances and critical questions. *Geological Society, London, Special Publications*, *390*(1), 9–43. https://doi.org/10.1144/SP390.25

Fossen, H. (1992). The role of extensional tectonics in the Caledonides of south Norway. *Journal of Structural Geology*, *14*(8-9), 1033–1046. https://doi.org/10.1016/0191-8141(92)90034-T

Fossen, H., & Cavalcante, G. C. G. (2017). Shear zones—A review. *Earth-Science Reviews*, *171*, 434–455. https://doi.org/10.1016/j.earscirev.2017.05.002

Fossen, H., & Dunlap, W. J. (1998). Timing and kinematics of Caledonian thrusting and extensional collapse, southern Norway: evidence from $^{40}Ar/^{39}Ar$ thermochronology. *Journal of Structural Geology*, *20*(6), 765–781. https://doi.org/10.1016/S0191-8141(98)00007-8

Fountain, D. M., Boundy, T. M., Austrheim, H., & Rey, P. (1994). Eclogite-facies shear zones—Deep crustal reflectors? *Tectonophysics*, *232*(1-4), 411–424. https://doi.org/10.1016/0040-1951(94)90100-7

Fusseis, F., Regenauer-Lieb, K., Liu, J., Hough, R. M., & De Carlo, F. (2009). Creep cavitation can establish a dynamic granular fluid pump in ductile shear zones. *Nature*, *459*(7249), 974–977. https://doi.org/10.1038/nature08051

Glodny, J., Kühn, A., & Austrheim, H. (2002). Rb/Sr record of fluid-rock interaction in eclogites, Bergen Arcs, Norway. *Geochimica et Cosmochimica Acta*, *66*, A280. https://doi.org/10.1016/S0016-7037(03)00370-3

Glodny, J., Kühn, A., & Austrheim, H. (2008). Geochronology of fluid-induced eclogite and amphibolite facies metamorphic reactions in a subduction–collision system, Bergen Arcs, Norway. *Contributions to Mineralogy and Petrology*, *156*(1), 27–48. https://doi.org/10.1007/s00410-007-0272-y

Godard, G., & van Roermund, H. L. M. (1995). Deformation-induced clinopyroxene fabrics from eclogites. *Journal of Structural Geology*, *17*(10), 1425–1443. https://doi.org/10.1016/0191-8141(95)00038-F

Griffin, W. L. (1972). Formation of eclogites and the coronas in anorthosites, Bergen Arcs, Norway. *Geological Society of America Memoirs*, *135*, 37–63. https://doi.org/10.1130/MEM135-p37

Hacker, B. R., Andersen, T. B., Johnston, S., Kylander-Clark, A. R. C., Peterman, E. M., Walsh, E. O., & Young, D. (2010). High-temperature deformation during continental-margin subduction & exhumation: The ultrahigh-pressure Western Gneiss Region of Norway. *Tectonophysics*, *480*(1-4), 149–171. https://doi.org/10.1016/j.tecto.2009.08.012

Halpaap, F., Rondenay, S., & Ottemöller, L. (2018). Seismicity, deformation, and metamorphism in the Western Hellenic subduction zone: New constraints from tomography. *Journal of Geophysical Research: Solid Earth*, *123*, 3000–3026. https://doi.org/10.1002/2017JB015154

Jackson, J. A., Austrheim, H., McKenzie, D., & Priestley, K. (2004). Metastability, mechanical strength, and the support of mountain belts. *Geology*, *32*(7), 625–628. https://doi.org/10.1130/G20397.1

Jakob, J., Alsaif, M., Corfu, F., & Andersen, T. B. (2017). Age and origin of thin discontinuous gneiss sheets in the distal domain of the magma-poor hyperextended pre-Caledonian margin of Baltica, southern Norway. *Journal of the Geological Society*, *174*(3), 557–571. https://doi.org/10.1144/jgs2016-049

Jamtveit, B., Austrheim, H., & Malthe-Sorenssen, A. (2000). Accelerated hydration of the Earth's deep crust induced by stress perturbations. *Nature*, *408*(6808), 75–78. https://doi.org/10.1038/35040537

Jamtveit, B., Ben-Zion, Y., Renard, F., & Austrheim, H. (2018). Earthquake-induced transformation of the lower crust. *Nature*, *556*(7702), 487–491. https://doi.org/10.1038/s41586-018-0045-y

Jamtveit, B., Bucher-Nurminen, K., & Austrheim, H. (1990). Fluid controlled eclogitization of granulites in deep crustal shear zones, Bergen arcs, Western Norway. *Contributions to Mineralogy and Petrology*, *104*(2), 184–193. https://doi.org/10.1007/BF00306442

Jamtveit, B., Moulas, E., Andersen, T. B., Austrheim, H., Corfu, F., Petley-Ragan, A., & Schmalholz, S. M. (2018). High pressure metamorphism caused by fluid induced weakening of deep continental crust. *Scientific Reports*, *8*(1), 17011. https://doi.org/10.1038/s41598-018-35200-1

Jeffery, G. B. (1922). The motion of ellipsoidal particles immersed in a viscous fluid. *Proceedings of the Royal Society of London A*, *102*(715), 161–179.

John, T., & Schenk, V. (2003). Partial eclogitisation of gabbroic rocks in a late Precambrian subduction zone (Zambia): Prograde metamorphism triggered by fluid infiltration. *Contributions to Mineralogy and Petrology*, *146*(2), 174–191. https://doi.org/10.1007/s00410-003-0492-8

Jolivet, L., Raimbourg, H., Labrousse, L., Avigad, D., Leroy, Y., Austrheim, H., & Andersen, T. B. (2005). Softening triggered by eclogitization, the first step toward exhumation during continental subduction. *Earth and Planetary Science Letters*, *237*(3–4), 532–547. https://doi.org/10.1016/j.epsl.2005.06.047

Keppler, R., Behrmann, J. H., & Stipp, M. (2017). Textures of eclogites and blueschists from Syros island, Greece: Inferences for elastic anisotropy of subducted oceanic crust. *Journal of Geophysical Research: Solid Earth*, *122*, 5306–5324. https://doi.org/10.1002/2017JB014181

Keppler, R., Ullemeyer, K., Behrmann, J. H., Stipp, M., Kurzawski, R. M., & Lokajíček, T. (2015). Crystallographic preferred orientations of exhumed subduction channel rocks from the Eclogite Zone of the Tauern Window (Eastern Alps, Austria), and implications on rock elastic anisotropies at great depths. *Tectonophysics*, *647-648*, 89–104. https://doi.org/10.1016/j.tecto.2015.02.011

Krogh, E. J. (1977). Evidence of Precambrian continent–continent collision in Western Norway. *Nature*, *267*(5606), 17–19. https://doi.org/10.1038/267017a0

Kufner, S.-K., Schurr, B., Haberland, C., Zhang, Y., Saul, J., Ischuk, A., & Oimahmadov, I. (2017). Zooming into the Hindu Kush slab breakoff: A rare glimpse on the terminal stage of subduction. *Earth and Planetary Science Letters*, *461*, 127–140. https://doi.org/10.1016/j.epsl.2016.12.043

Kühn, A., Glodny, J., Austrheim, H., & Råheim, A. (2002). The Caledonian tectono-metamorphic evolution of the Lindås Nappe: Constraints from U-Pb, Sm-Nd and Rb-Sr ages of granitoid dykes. *Norsk Geologisk Tidsskrift*, *82*, 45–57.

Labrousse, L., Hetényi, G., Raimbourg, H., Jolivet, L., & Andersen, T. B. (2010). Initiation of crustal-scale thrusts triggered by metamorphic reactions at depth: Insights from a comparison between the Himalayas and Scandinavian Caledonides. *Tectonics*, *29*, TC5002. https://doi.org/10.1029/2009TC002602

Lloyd, G. E., Halliday, J. M., Butler, R. W. H., Casey, M., Kendall, J.-M., Wookey, J., & Mainprice, D. (2011). From crystal to crustal: Petrofabric-derived seismic modelling of regional tectonics. *Geological Society, London, Special Publications*, *360*(1), 49–78. https://doi.org/10.1144/SP360.4

Maggi, M., Rosetti, F., Corfu, F., Theye, T., Andersen, T. B., & Faccenna, C. (2012). Clinopyroxene–rutile phyllonites from the East Tenda Shear Zone (Alpine Corsica, France): Pressure–temperature–time constraints to the Alpine reworking of Variscan Corsica. *Journal of the Geological Society*, *169*(6), 723–732. https://doi.org/10.1144/jgs2011-120

Mavko, G., Mukerji, T., & Dvorkin, J. (2009). *The rock physics handbook*, (2nd ed.). Cambridge, UK: Cambridge Univ. Press. https://doi.org/10.1017/CBO9780511626753

Mørk, M. B. E. (1985). A gabbro to eclogite transition on Flemsøy, Sunnmøre, western Norway. *Chemical Geology*, *50*(1-3), 283–310. https://doi.org/10.1016/0009-2541(85)90125-1

Motra, H. B., & Zertani, S. (2018). Influence of loading and heating processes on elastic and geomechanical properties of eclogites and granulites. *Journal of Rock Mechanics and Geotechnical Engineering*, *10*(1), 127–137. https://doi.org/10.1016/j.jrmge.2017.11.001

Passchier, C. W., & Simpson, C. (1986). Porphyroclast systems as kinematic indicators. *Journal of Structural Geology*, *8*(8), 831–843. https://doi.org/10.1016/0191-8141(86)90029-5

Petley-Ragan, A., Dunkel, K. G., Austrheim, H., Ildefonse, B., & Jamtveit, B. (2018). Microstructural records of earthquakes in the lower crust and associated fluid-driven metamorphism in plagioclase-rich granulites. *Journal of Geophysical Research: Solid Earth*, *123*, 3729–3746. https://doi.org/10.1029/2017JB015348

Plümper, O., Botan, A., Los, C., Liu, Y., Malthe-Sørenssen, A., & Jamtveit, B. (2017). Fluid-driven metamorphism of the continental crust governed by nanoscale fluid flow. *Nature Geoscience*, *10*(9), 685–690. https://doi.org/10.1038/ngeo3009

Pollok, K., Lloyd, G. E., Austrheim, H., & Putnis, A. (2008). Complex replacement patterns in garnets from Bergen Arcs eclogites: A combined EBSD and analytical TEM study. *Chemie der Erde*, *68*(2), 177–191. https://doi.org/10.1016/j.chemer.2007.12.002

Putnis, A., Jamtveit, B., & Austrheim, H. (2017). Metamorphic processes and seismicity: The Bergen arcs as a natural laboratory. *Journal of Petrology*, *58*(10), 1871–1898. https://doi.org/10.1093/petrology/egx076

Putnis, A., & John, T. (2010). Replacement processes in the Earth's crust. *Elements*, *6*(3), 159–164. https://doi.org/10.2113/gselements.6.3.159

Raimbourg, H., Goffé, B., & Jolivet, L. (2007). Garnet reequilibration and growth in the eclogite facies and geodynamical evolution near peak metamorphic conditions. *Contributions to Mineralogy and Petrology*, *153*(1), 1–28. https://doi.org/10.1007/s00410-006-0130-3

Raimbourg, H., Jolivet, L., Labrousse, L., Leroy, Y., & Avigad, D. (2005). Kinematics of syneclogite deformation in the Bergen arcs, Norway: Implications for exhumation mechanisms. *Geological Society, London, Special Publications*, *243*(1), 175–192. https://doi.org/10.1144/GSL.SP.2005.243.01.13

Roberts, D. (2003). The Scandinavian Caledonides: Event chronology, palaeogeographic settings and likely modern analogues. *Tectonophysics*, *365*(1-4), 283–299. https://doi.org/10.1016/S0040-1951(03)00026-X

Roberts, D., & Gee, D. G. (1985). An introduction to the structure of the Scandinavian Caledonides. In D. G. Gee, & B. A. Sturt (Eds.), *The Caledonide Orogen—Scandinavia and related areas* (Vol. 1, pp. 55–68). Chichester: John Wiley.

Roffeis, C., Corfu, F., & Austrheim, H. (2012). Evidence for a Caledonian amphibolite to eclogite facies pressure gradient in the Middle Allochthon Lindås Nappe, SW-Norway. *Contributions to Mineralogy and Petrology*, *164*(1), 81–99. https://doi.org/10.1007/s00410-012-0727-7

Schmid, R., Altenberger, U., & Oberhänsli, R. (1998). *Polyphase tectono-metamorphic evolution of the northwestern Lindas Nappe on Holsnoy*. Caledonides, SW-Norway: Bergen Arcs.

Schrank, C. E., Handy, M. R., & Fusseis, F. (2008). Multiscaling of shear zones and the evolution of the brittle-to-viscous transition in continental crust. *Journal of Geophysical Research*, *113*, B01407. https://doi.org/10.1029/2006JB004833

Sturt, B. A., Skarpenes, O., Ohanian, A. T., & Pringle, I. R. (1975). Reconnaissance Rb/Sr isochron study in the Bergen Arc System and regional implications. *Nature*, *253*(5493), 595–599. https://doi.org/10.1038/253595a0

Wain, A. L., Waters, D. J., & Austrheim, H. (2001). Metastability of granulites and processes of eclogitisation in the UHP region of western Norway. *Journal of Metamorphic Geology*, *19*(5), 609–625. https://doi.org/10.1046/j.0263-4929.2001.00333.x

Wayte, G. J., Worden, R. H., Rubie, D. C., & Droop, G. T. R. (1989). A TEM study of disequilibrium plagioclase breakdown at high pressure: The role of infiltrating fluid. *Contributions to Mineralogy and Petrology*, *101*(4), 426–437. https://doi.org/10.1007/BF00372216

Zhong, X., Frehner, M., Kunze, K., & Zappone, A. (2014). A novel EBSD-based finite-element wave propagation model for investigating seismic anisotropy: Application to Finero Peridotite, Ivrea-Verbano Zone, Northern Italy. *Geophysical Research Letters*, *41*, 7105–7114. https://doi.org/10.1002/2014GL060490